Article

Modeling As(III) oxidation and removal with iron electrocoagulation in groundwater

lei li, Case Michael van Genuchten, Susan E. A. Addy, Juanjuan Yao, Naiyun Gao, and Ashok Gadgil

Environ. Sci. Technol., **Just Accepted Manuscript** • Publication Date (Web): 17 Sep 2012

Modeling As(III) oxidation and removal with iron electrocoagulation in groundwater

Lei Li[1,2], Case M. van Genuchten[2], Susan E. A. Addy[2],*

Juanjuan Yao[3], Naiyun Gao[1], Ashok J. Gadgil[2,4]

[1]Current Address: State Key Laboratory of Pollution Control and Resources Reuse, College of Environmental Science and Engineering, Tongji University, Shanghai 200092, China

[2]Department of Civil and Environmental Engineering, University of California, Berkeley, Berkeley, California 94720, USA.

[3]Key Laboratory of the Three Gorges Reservoir Eco-Environment, Ministry of Education, Chongqing University, Chongqing, 400045, China

[4]Environmental Energy Technologies Division, Lawrence Berkeley National Laboratory, Berkeley, California 94720, USA.

*Corresponding author.

Email addresses: susan.e.addy@gmail.com

Keywords: Iron electrocoagulation, arsenic removal, sustainable water treatment, groundwater

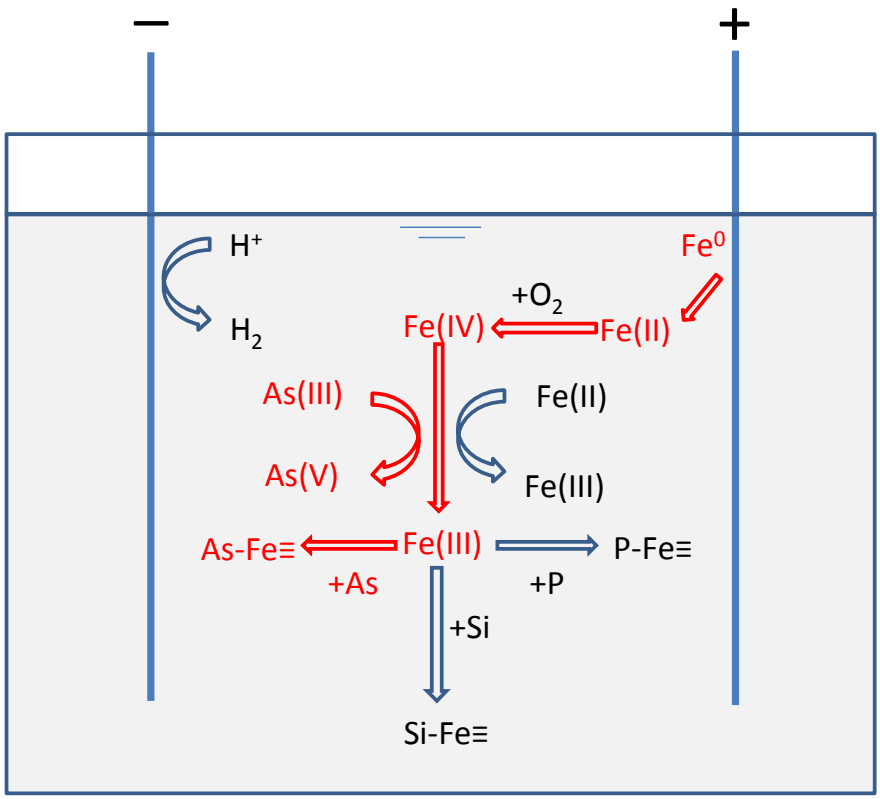
−
+
H+
H2
Fe0
+O2
Fe(IV)
Fe(II)
As(III)
As(V)
Fe(II)
Fe(III)
As-Fe≡
Fe(III)
P-Fe≡
+As
+P
+Si
Si-Fe≡

TOC Image

Abstract

Understanding the chemical kinetics of arsenic during electrocoagulation (EC) treatment is essential for a deeper understanding of arsenic removal using EC under a variety of operating conditions and solution compositions. We describe a highly-constrained, simple chemical dynamic model of As(III) oxidation and As(III,V), Si, and P sorption for the EC system using model parameters extracted from some of our experimental results and previous studies. Our model predictions agree well with both data extracted from previous studies and our observed experimental data over a broad range of operating conditions (charge dosage rate) and solution chemistry (pH, co-occurring ions) without free model parameters. Our model provides insights into why higher pH and lower charge dosage rate (Coulombs/L/min) facilitate As(III) removal by EC, and sheds light on the debate in the recent published literature regarding the mechanism of As(III) oxidation during EC. Our model also provides practically useful estimates of the minimum amount of iron required to remove 500 μg/L As(III) to < 50 μg/L. Parameters measured in this work include the ratio of rate constants for Fe(II) and As(III) reactions with Fe(IV) in synthetic groundwater (k_1/k_2 = 1.07) and the apparent rate constant of Fe(II) oxidation with dissolved oxygen at pH 7 ($k_{app} = 10^{0.22}$ $M^{-1}s^{-1}$).

1. Introduction

Chronic exposure to toxic levels of naturally occurring arsenic in drinking water is a major public health problem threatening the lives of over 140 million people worldwide[1]. Arsenic contamination has brought tens of thousands of people cancer of the skin and internal organs[1, 2] and by one recent estimate might account for roughly 20% of deaths in Bangladesh[3]. The United States Environmental Protection Agency (USEPA) and the World Health Organization (WHO) have reduced the maximum recommended arsenic level in drinking water from 50 to 10 μg/L[4, 5].

Among the typical iron-based techniques used to remediate arsenic-contaminated water, electrocoagulation (EC) using Fe(0) electrodes has the potential to be one of the most efficient and cost-effective[6, 7]. EC systems are easy to operate and maintain, produce less waste than other coagulation methods[8], and, perhaps most important to sustainable operation in rural areas, can be implemented and operated with only relatively low levels of technical skill and small inputs of locally available materials[9, 10]. EC is based on the production of Fe(II)[7] through the electrolytic dissolution of an Fe(0) anode (Eq. (1)). The reaction occurring at the cathode is frequently cited as H^+ reduction to H_2 gas[7, 11, 12] (Eq. (2)), though we note that detailed electrochemical studies were beyond the scope of this work (refer to Eq. (1) and (2) for electrochemical equations).

$$Fe(0) \rightarrow Fe(II) + 2e^- \ldots (1)$$

$$2H^+ + 2e^- \rightarrow H_{2(g)} \ldots (2)$$

The generated Fe(II) is rapidly oxidized by dissolved oxygen (DO) in aerated solutions, leading to the formation of reactive hydrous ferric oxide (HFO) precipitates with a high arsenic sorption affinity[7]. EC has several unique benefits unavailable in conventional iron-based approaches (e.g.

iron oxide coated sand filters, Fe(II) or Fe(III) salt addition, passive Fe(0) corrosion). For example, the externally applied current, and thus the higher rate of Fe(II) production, can shorten the treatment time compared to natural corrosion of $Fe(0)/O_2$ systems. The typical observed drop in pH following Fe(II) oxidation and Fe(III) hydrolysis in chemical coagulation (CC) systems (e.g. $FeSO_4$) can be buffered in the EC system by the evolution of $H_{2(g)}$ occurring at the cathode (Eq. (2)). Buffering of pH also gives EC an advantage over other techniques that may require pH adjustment in the final step, such as lime softening or alum coagulation[13]. There is also broad agreement in the literature that a major benefit of EC is its effective oxidation of arsenite, or As(III). Because arsenate, or As(V), has a higher affinity for the surface of HFO, overall arsenic removal can be enhanced by the oxidation of As(III)[14-17], which is often the predominant form of arsenic in groundwater[18].

Although arsenic removal using EC has been previously explored[6, 19-23], detailed studies of As(III) oxidation and As(III,V) adsorption in EC systems are largely absent from the literature. Furthermore, several conflicting theories regarding the mechanism of As(III) oxidation in EC systems are described in the literature. For example, a 2010 paper proposes electrocatalytic As(III) oxidation via direct electron transfer with anode[19]. Another paper, also in 2010, proposes Cl_2 mediated As(III) oxidation through anodic production of Cl_2 from Cl^- [24]. A third paper, in the same year, proposes As(III) oxidation by reactive oxidant species generated during the simultaneous oxidation of Fe(II) by DO[25]. Not only do we provide results serving to resolve this debate, we also rigorously investigate the chemical reactions responsible for the oxidation of

As(III) in EC systems. Additionally, only a few models of As(III,V) removal have been developed for the Fe(II)/O_2 chemical coagulation system in groundwater of similar composition to that of the target region of West Bengal (India) and Bangladesh[14]. Because EC systems include additional operating parameters, such as the rate of Fe(II) production, the results of previous As(III) oxidation studies in the Fe(II)/O_2 and Fe(II)/H_2O_2 chemical coagulation systems[26] will not likely provide a complete description of As(III) removal. Accordingly, we developed a highly-constrained chemical dynamic model of As(III) oxidation and As(III,V) sorption for the EC system using model parameters extracted from our experimental results as well as previous studies[14]. Our model reproduces both our observed data and data extracted from a previous study[14] over a broad range of operating conditions (charge dosage rate) and solution chemistry (pH, co-occurring ions) without free model parameters. Our model also provides estimates of the minimum amount of iron required to remove 500 μg/L As(III) to < 50 μg/L in synthetic groundwater under a range of practical conditions, and thus it can be a useful tool for operating and maintaining efficient EC systems in the field.

2. Methods

Synthetic Groundwater. All chemicals used in experiments ($NaAsO_2$, $Na_2HAsO_4 \cdot 7H_2O$, Na_2HPO_4, $Na_2SiO_3 \cdot 9H_2O$, $FeSO_4 \cdot 7H_2O$, $Fe(NO_3)_3$, $CaCl_2$, $MgCl_2$, $NaBH_4$, NaOH, KI, ascorbic acid, disodium citrate, and 2,2′-bipyridine) were reagent grade or higher. Experiments were carried out in synthetic Bangladesh groundwater (SBGW), which has a composition based on a

comprehensive British Geological Survey (BGS) analysis of groundwater wells in Bangladesh[14, 18]. Unless otherwise noted, SBGW contains 8.2 mM $NaHCO_3$, 2.5 mM $CaCl_2$, 1.6 mM $MgCl_2$, 500 µg/L As(III), 3 mg/L NaH_2PO_4-P and 30 mg/L Na_2SiO_3-Si. Batches of SBGW were prepared by adding $NaHCO_3$, $MgCl_2$, Na_2HPO_4, and Na_2SiO_3 as solids to ultrapure 18 MΩ water in sequence under vigorous stirring. The pH was then reduced to ~8 by bubbling $CO_{2(g)}$. $CaCl_2$ stock solution (5% w/v) was added subsequently. Arsenic was added before adjusting pH to 7.0 by bubbling $CO_{2(g)}$. All batches were aged at least 1h after all components had been added and then sampled to verify the initial concentrations of P, Si, As(III), and As(tot).

Arsenic Speciation and Wet Chemical Analysis. As(III) and As(tot) were determined using an inductively coupled plasma optical emission system with hydride generation (HG-ICP, Perkin Elmer5300 DV). To selectively detect As(III), we followed the procedures outlined in Roberts et al.[14]. P, Si and Fe(tot) were also determined with the same instrument (without hydride generation). The relative standard deviation (RSD) for the detection of all elements was < 10% (typically < 4%). A ferrozine method was used to determine the concentration of aqueous and total Fe(II)[27].

Oxidation/Adsorption Experimental Set Up. Experiments were conducted in a 1 L beaker using 5x11 cm^2 Fe(0) steel plate electrodes separated by approximately 7.5 cm. All glassware used in experiments and sample collection was soaked in 10% HNO_3 and rinsed with DI water prior to use. The active area of the Fe(0) anode was held constant while the operating current was adjusted to achieve the desired charge dosage rate. The iron dosage rate (D, g

Fe/min/L) is related to the charge dosage rate (Q, Coulombs/L/min) through Faraday's law (Eq. (3)),

$$D = Q\left(\frac{M}{Z \cdot F}\right) = \frac{i}{V}\left(\frac{M}{Z \cdot F}\right) \ldots (3)$$

where M is the molecular weight of iron (g/mol), Z is the number of electrons involved (equivalents/mol), and F is Faraday's constant (Coulombs/mol). According to Eq. (3), Q (and thus, D) is set by defining the current, i (Coulombs/s), given the volume, V (L), of electrolyte. Since the iron dosage (D) and charge dosage (Q) rates are proportional, these terms are exchangeable in the subsequent discussion of our model. Our model (described below) assumes Fe(II) is generated at 100% of the theoretical (Faradaic) value. A digital multimeter (Agilent, 34410A) was used to verify the operating current supplied by a DC power supply (HP, E3631A). The surface of the Fe(0) anode was mechanically cleaned prior to experiments to remove any passive film that may have formed. Samples (25ml) were taken from the reactor using a wide-tipped syringe immediately following the electrolysis and stirred in a separate beaker for 2h. A first set of samples was filtered through 0.45 μm nylon filters for the determination of filterable (herein referred to as aqueous) As, P, and Si. A second set of unfiltered samples was taken and digested in HCl before analysis for the determination of total As, P, or Si. The adsorbed fraction was then calculated as the difference between the two measurements. A teflon-coated magnetic stirrer was used during the electrolysis and reaction stages of treatment to ensure adequate mixing. In preliminary experiments, the pH increased 0.2 to 0.6 units after the electrolysis stage likely due to release of $CO_{2(g)}$. Therefore, pH drift was minimized (± 0.1 units) during the electrolysis and

reaction stages by carefully bubbling $CO_{2(g)}$ intermittently throughout treatment. Because all experiments were carried out open to the atmosphere, the brief, sporadic bubbling of $CO_{2(g)}$ to maintain pH was not sufficient to purge DO from solution. All experiments were conducted at room temperature (23±2°C).

As(III) Oxidation and Adsorption Model Equations. A chemical dynamic model of As(III) oxidation and As(III,V) adsorption was developed based on previous detailed studies of the Fe(II)/O_2 system[26, 28]. Equations (1-17) (shown in Table 1 and explained below) form the basis for this simplified model describing the EC process.

Fe(IV) was used in this study to represent the oxidant produced in the EC system because it is generally accepted as the intermediate oxidant in the Fe(II)/O_2 system at neutral pH[26, 29, 30]. Fe(IV) is generated from Fe(II) oxidation through several steps (Eq. (4-7)), with the reaction in Eq. (4) likely serving as the rate limiting step[26].

$$Fe(II) + O_2 \rightarrow O_2^{\cdot -} + Fe(III) \ldots (4)$$

$$Fe(II) + O_2^{\cdot -} + 2H^+ \rightarrow Fe(III) + H_2O_2 \ldots (5)$$

$$Fe(II) + H_2O_2 \rightarrow intermediate\ (INT) \ldots (6)$$

$$(INT) \rightarrow Fe(IV) \ldots (7)$$

Using the generic pathways described in Eq. (4-7) we can describe the production of Fe(IV) in Eq. (8), which indicates that generating 1 mol Fe(IV) requires 3 mol of oxidized Fe(II).

$$3Fe(II) + O_2 \rightarrow Fe(IV) + 2Fe(III) \ldots (8)$$

Following the approach of Hug et al. 2003[26], our model assumes that the majority of the generated Fe(IV) goes on to be consumed in oxidation reactions with either Fe(II) (Eq. (9)), or As(III) (Eq. (10).

$$Fe(IV) + Fe(II) \longrightarrow 2Fe(III) \qquad k_1 \quad \ldots(9)$$

$$Fe(IV) + As(III) \longrightarrow Fe(III) + As(IV) \qquad k_2 \quad \ldots(10)$$

Therefore, the change of Fe(IV) with time (d[Fe(IV)]/dt; Eq. (9 and 10)) is partly determined by Fe(II) and As(III) oxidation reactions. However, due to the high relative abundance of Fe(II) during EC in SBGW, the fraction of Fe(IV) consumed by As(III) is much less than the fraction consumed by Fe(II). Accordingly, if we assume that Fe(IV) goes on to oxidize Fe(II), then, using Eq. (8), the amount of Fe(IV) that was generated is related to the amount of Fe(II) oxidized. Therefore, we introduce a coefficient of proportionality, ß (Eq. (11)), having a value of ¼ assuming k_2[As(III)] is orders of magnitude less than k_1[Fe(II)].

$$[Fe(IV)] = \beta[Fe(II)]_{oxidation} \ldots (11)$$

The fraction of Fe(IV) that goes on to react with As(III) ($R_{Fe(IV)\rightarrow As(III)}$)) is expressed by Eq. (12),

$$R_{Fe(IV)\rightarrow As(III)} = \frac{1}{1+\frac{k_1[Fe(II)]}{k_2[As(III)]}} \ldots (12)$$

where k_1 and k_2 are the respective rate constants for Fe(II) and As(III) oxidation by Fe(IV). The oxidation rate of As(III) is expressed by Eq. (13),

$$\frac{d[As(III)]_{oxidation}}{dt} = R_{Fe(IV)\rightarrow As(III)} \cdot \frac{d[Fe(IV)]}{dt} = \frac{\beta}{1+\frac{k_1[Fe(II)]}{k_2[As(III)]}} \frac{d[Fe(II)]_{oxidation}}{dt} \quad \ldots (13)$$

where $R_{Fe(IV)\rightarrow As(III)}$ is given in Eq. (12), and Fe(IV) is given in Eq. (11). The overall rate of Fe(II) oxidation is given in Eq. (14),

$$\frac{d[Fe(II)]_{oxidation}}{dt} = -k_{app}[Fe(II)][O_2] \ldots (14)$$

$$k_{app} = \left((k_{Fe^{2+}} \cdot \alpha_{Fe^{2+}}) + (k_{FeOH^+} \cdot \alpha_{FeOH^+}) + \left(k_{Fe(OH)_2^0} \cdot \alpha_{Fe(OH)_2^0}\right) + \cdots\right)$$

where k_{app} is the apparent rate constant of Fe(II) oxidation. Equation (14) indicates that the apparent Fe(II) oxidation rate is largely influenced by Fe(II) speciation with corresponding pH dependence and equals a weighted sum of the oxidation rates of all possible aqueous Fe(II) species. The adsorption of As(III) is given in Eq. (15),

$$[As(III)]_{adsorption} = \frac{q_{max}[Fe(III)]K_{As(III)}[As(III)]}{1+K_{As(III)}[As(III)]+K_{As(V)}[As(V)]+K_P[P]+K_{Si}[Si]} \ldots (15)$$

where q_{max} is the adsorption capacity, [Fe(III)] is the concentration of HFO, and $K_{As(III)}$, $K_{As(V)}$, K_P, and K_{Si} are the adsorption equilibrium constants for the competitive adsorption of As(III), As(V), P, and Si, respectively. Adsorption equilibrium constants and adsorption capacity values measured in our EC system at D = 3 and 24 Coulombs/L/min were within experimental error of those measured in a similar CC system[14]. Knowing the expressions for As(III) adsorbed (Eq. (15)) and As(III) oxidized (Eq. (13)), we can express the final As(III) concentration after treatment by Eq. (16).

$$[As(III)]_{final} = [As(III)]_{initial} - [As(III)]_{oxidation} - [As(III)]_{adsorption} \ldots (16)$$

Here we neglect any As(III) adsorbed to the electrode surface based on preliminary recovery tests (> 90%). Consistent with Roberts et al.[14], our model treats the EC system as homogeneous. Any adsorbed As(III), Fe(II), Fe(IV), O_2, H_2O_2, and $O_2^{\cdot-}$ were treated as aqueous species with respect to their oxidation kinetics. This assumption is based on their low sorption affinity to HFO. In our

model, As(III) oxidation is dependent on DO, Fe(II), pH and $R_{As(III)/Fe(II)}$. As(III) adsorption is proportional to q_{max}, HFO concentration and the concentration of competing ions, especially PO_4^{3-} and As(V), which have orders of magnitude higher sorption affinity to HFO than As(III)[14, 31, 32]. Finally, we ignored any potential electrocatalytic reactions that might oxidize As(III) (anodic Cl_2 production or direct anodic As(III) oxidation) because As(III) oxidation during electrolysis was negligible if Fe(II) oxidation was suppressed by the addition of 3mM 2,2′-bipyridine, consistent with Katsoyiannis et al.[28]. All model predictions were carried out using Mathematica 7.0 [33].

Determination of Selected Reaction Constants and Model Parameters. Before applying our proposed model to the EC system, the ratio of rate constants for Fe(II) and As(III) oxidation by Fe(IV) (k_1/k_2) and the apparent rate constant of Fe(II) oxidation (k_{app}) were determined by measuring the rates of Fe(II) and As(III) oxidation after adding Fe(II) and As(III) salts to aerated SBGW (Figure S2 of supporting information). The value of k_1/k_2 (Eq. 9, 10) was found to be 1.07, indicating that the rate of As(III) and Fe(II) oxidation by Fe(IV) are of similar orders of magnitude in SBGW. The value of k_{app} (Eq. (13)) at pH 7.0 was found to be $10^{0.22}$ $M^{-1}s^{-1}$, which matches well with reported values[26, 34] (Table 1). It should be reiterated here that k_{app} bears strong pH dependence in both k_x and α_x of Eq. (14). The pH-dependence of k_{app} was input into the model based on the assumption that $Fe(OH)_2^0$ is the dominant Fe(II) species being oxidized, consistent with previous work [28, 35].

In an additional, separate experiment, we verified the proposed stoichiometry of Fe(IV) production applied in our model (Eq. (8)), which is described further in the supporting information.

Computational Model. Equations (4-17) were turned into a computational predictive model based on a forward time-marching finite difference scheme, implemented to first order differencing accuracy, written in Mathematica. The start of electrolysis was designated as time t = 0. For a given model experiment, the dosage rate D was constant until the end of electrolysis, at which point D was set to 0 for the remaining reaction time (2h).

Table 1: Reactions in the EC system.

Number	Reaction	
(1)	$Fe(0) \rightarrow Fe(II) + 2e^-$	
(2)	$2H^+ + 2e^- \rightarrow H_{2(g)}$	
(3)	$D = Q\left(\frac{M}{Z \cdot F}\right) = \frac{i}{V}\left(\frac{M}{Z \cdot F}\right)$	
(4)	$Fe(II)+O_2 \rightarrow O_2^{\cdot-}+Fe(III)$	
(5)	$Fe(II)+ O_2^{\cdot-} +2H^+ \rightarrow Fe(III)+H_2O_2$	
(6)	$Fe(II)+ H_2O_2 \rightarrow$ intermediate(INT)	
(7)	INT→Fe(IV)	
(8)	$3Fe(II)+O_2 \rightarrow Fe(IV)+2Fe(III)$	
(9)	Fe(IV)+ Fe(II)→ 2Fe(III), $\frac{d[Fe(II)]}{dt} = -k_1[Fe(II)][Fe(IV)]$ $\frac{d[\mathrm{Fe(II)}]}{dt}$=$k_1$[Fe(II)][Fe(IV)]	k_1
(10)	Fe(IV)+ As(III)→ Fe(III)+ As(IV), $\frac{d[As(III)]}{dt} = -k_2[As(III)][Fe(IV)]$ $\frac{d[\mathrm{As(III)}]}{dt}$=$k_2$[As(III)][Fe(IV)]	k_2
(11)	$[Fe(IV)] = \beta[Fe(II)]_{oxidation}$	β ≈ 0.25
(12)	$R_{Fe(IV)\rightarrow As(III)} = \frac{1}{1+\frac{k_1[Fe(II)]}{k_2[As(III)]}}$	
(13)	$\frac{d[As(III)]_{oxidation}}{dt} = R_{Fe(IV)\rightarrow As(III)} \cdot \frac{d[Fe(IV)]}{dt} = \frac{\beta}{1+\frac{k_1[Fe(II)]}{k_2[As(III)]}} \frac{d[Fe(II)]_{oxidation}}{dt}$	$\frac{k_1}{k_2}$=1.07
(14)	$\frac{d[Fe(II)]_{oxidation}}{dt} = -k_{app}[Fe(II)][O_2]$ $k_{app} = \left((k_{Fe^{2+}} \cdot \alpha_{Fe^{2+}}) + (k_{FeOH^+} \cdot \alpha_{FeOH^+}) + \left(k_{Fe(OH)_2^0} \cdot \alpha_{Fe(OH)_2^0}\right) + \cdots\right)$	$\log k_{app}$ = 0.22 (pH=7.0±0.1),
(15)	$[As(III)]_{adsorption} = \frac{q_{max}[Fe(III)]K_{As(III)}[As(III)]}{1 + K_{As(III)}[As(III)] + K_{As(V)}[As(V)]+K_P[P] + K_{Si}[Si]}$	
(16)	$[As(III)]_{final} = [As(III)]_{initial} - [As(III)]_{oxidation} - [As(III)]_{adsorption}$	

$$\frac{d[Fe(II)]}{dt} = \frac{d[Fe(II)]_{oxidation}}{dt} + \frac{d[Fe(II)]_{dosage}}{dt} = -k_{app}[Fe(II)][O_2] + D \quad (17)$$

3. Result and Discussion

Effect of Iron/Charge Dosage Rate. Controlling the charge dosage rate can greatly improve the extent of As(III) oxidation in the EC system by increasing $R_{As(III)/Fe(II)}$. Because the sorption affinity of As(III) is much less than As(V), the removal of As(III) can be greatly enhanced if it is oxidized to As(V). The amount of Fe(II) remaining in solution (and thus $R_{As(III)/Fe(II)}$) is governed by the rate of Fe(II) oxidation and the iron dosage rate (D) (Eq.(17)).

$$\frac{d[Fe(II)]}{dt} = \frac{d[Fe(II)]_{oxidation}}{dt} + \frac{d[Fe(II)]_{dosage}}{dt} = -k_{app}[Fe(II)][O_2] + D \ldots (17)$$

At low charge dosage rates (e.g. 1 Coulombs/L/min), the rate of Fe(II) oxidation is nearly equal to the rate of Fe(II) production, leading to a low aqueous Fe(II) concentration (Figure 1a) and high $R_{As(III)/Fe(II)}$. The lower iron dosage rate improves As(III) oxidation and results in a much lower amount of iron required to decrease As(tot) < 50 μg/L (Figure 1b). Conversely, a high charge dosage rate (12 and 24 Coulombs/L/min) leads to an almost linear increase in aqueous Fe(II) with electrolysis time, resulting in a lower $R_{As(III)/Fe(II)}$ and lower As(III) oxidation. The highest reported iron dosage rates required nearly twice as much iron (~43 mg/L) as the lowest iron dosage rates, reflecting the importance of controlling As(III) oxidation. As charge dosage rate increases, the behavior of As(III) oxidation in EC becomes similar to CC, where Fe(II) is dosed at one time. Figure 1b indicates that the corresponding required iron levels off at ~45 - 50 mg/L as charge

dosage rate increases, which is consistent with previous CC studies (~50 mg/L) conducted in similar electrolytes[14].

A lower iron dosage rate is also beneficial because it is more likely to maintain a higher concentration of DO, which is necessary for efficient Fe(II) oxidation. At lower charge dosage rates, the rate of DO consumption from Fe(II) oxidation can be low enough to be easily offset by the flux of atmospheric oxygen into the stirred tank during treatment. On the other hand, the operation of EC systems at lower iron dosage rates can result in longer treatment times.

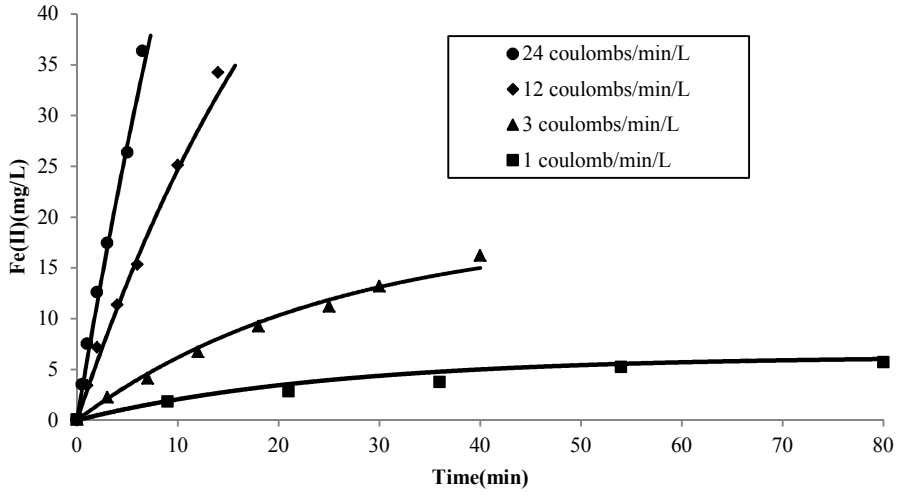

(a)

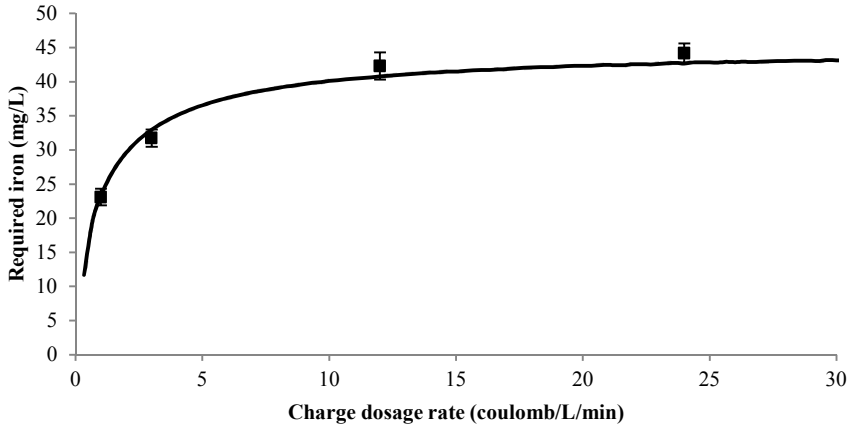

(b)

Figure 1: (a) Fe(II) concentration as a function of time for various charge dosage rates and (b) Minimum iron required for As removal from 500 to < 50 µg/L as a function of iron/charge dosage rate. Symbols are experimental data. Bars on symbols represent a range of observations in replicate experiments. The lines represent the output from the model calculation. Initial and final pH 7.1 ± 0.1.

Effect of pH on Adsorption and Oxidation. Due to the strong pH dependence of Fe(II) oxidation, pH is likely to influence $R_{As(III)/Fe(II)}$ and As(III) oxidation. Figure 2a verifies that an increase in pH benefits Fe(II) oxidation, consistent with previous work[35, 36]. As seen in Figure 2a, at pH 6.8, approximately 90% of total iron (~28 mg/L) exists as Fe(II) at the end of electrolysis. On the other hand, the concentration of Fe(II) remaining in solution after electrolysis at pH 7.6 is only 1-3 mg/L. Figure 2b shows the amount of total iron dose required to reduce As(tot) in SBGW from 500 µg/L to below 50 µg/L at pH values ranging from approximately 6.95 to 7.8. The

amount of iron required showed strong pH dependence, decreasing from approximately 48 mg/L at pH 6.95 to approximately 17 mg/L at pH 7.8. This large change in required iron can be understood per our simplified model as follows. At higher pH, Fe(II) is rapidly oxidized to Fe(III) soon after being generated, and in the process, oxidizes most of the As(III) to As(V) due to the minor competition of aqueous Fe(II) for the intermediate oxidant, following Eq. (4-10). As(V) is more readily adsorbed by HFO than As(III) and thus As(tot) decreases dramatically with only small inputs of Fe(tot). At lower pH, the slow oxidation rate of aqueous Fe(II) causes a brief accumulation of Fe(II), leading to greater competition for the intermediate oxidant. Accordingly, more As(tot) exists as As(III) after the complete oxidation of Fe(II) and more inputs of Fe(tot) are required to remove As(tot) due to the lower As(III) adsorption affinity.

The general trend of increasing required iron with decreasing pH is predicted by the model, represented by the solid line in Figure 2b. The sharp increase in required iron at the lower pH range shown in Figure 2b is due to the incomplete oxidation of Fe(II) in the 2 hr reaction stage. Due to the slow rate of Fe(II) oxidation at pH < 7.1, the amount of total iron generated by EC does not produce sufficient HFO because unoxidized Fe(II) remains in solution (Figure 2a). However, it is important to reiterate that the experiments in this study were carried out with a reaction stage of 2 hr to mimic treatment in the field. If ample time was given to allow for complete Fe(II) oxidation, the slope of the model prediction line in Figure 2b for pH < 7.1 is expected to be less steep, which is consistent with model predictions carried out at increasing mixing times. The three experimental data points and model predictions for the required iron are in reasonable

agreement for pH < 7.4; the differences between data and model predictions increase at higher pH. The exact differences between experimental data and model predictions are -8.3, -2.4, 3.2, 5.5, and 6.7 mg/L for pH 6.95, 7.1, 7.4, 7.6, and 7.8 respectively. Because our simplified model treats the precipitate surface as unchanging, the discrepancy in experimental data and model predictions might be explained by the pH dependence of As(V) adsorption to HFO surfaces. In transition from neutral to slightly alkaline pH, the HFO surface charge decreases from positive to negative, while during the same pH transition the dominant species of As(V) changes from $H_2AsO_4^-$ to the more negatively charged $HAsO_4^{2-}$ [31]. Thus the transition from neutral to a slightly alkaline pH leads to an increased electrostatic repulsion that can decrease the affinity of As(V) for HFO surfaces[37]. As a result, the iron required to remove aqueous As(tot) to < 50 µg/L determined experimentally was almost twice (~17 mg/L) the value predicted by our simplified model (~9 mg/L) at pH 7.8 (Figure 2b). Additionally, a change in pH can alter k_{app} and the overall rate of Fe(II) oxidation by changing the Fe(II) speciation. Because our model approximates the pH dependence of k_{app} using the pH dependence of $Fe(OH)_2^0$, a substantial variation in pH during the electrolysis or reaction stages might lead to substantial errors in model predictions of As(III) oxidation and removal. Since k_{app} was measured at pH 7.0, it makes sense that there is more agreement at neutral pH. The ratio k1/k2 will also have some pH dependence that has not been modeled here. A more rigorous description of the pH-dependent reactions involved in the oxidation and removal of As(III) is beyond the scope of this work.

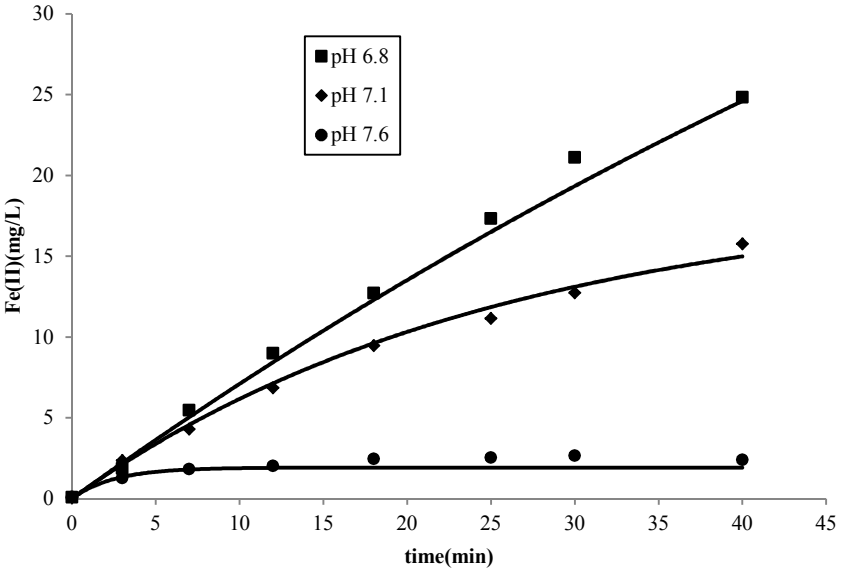

(a)

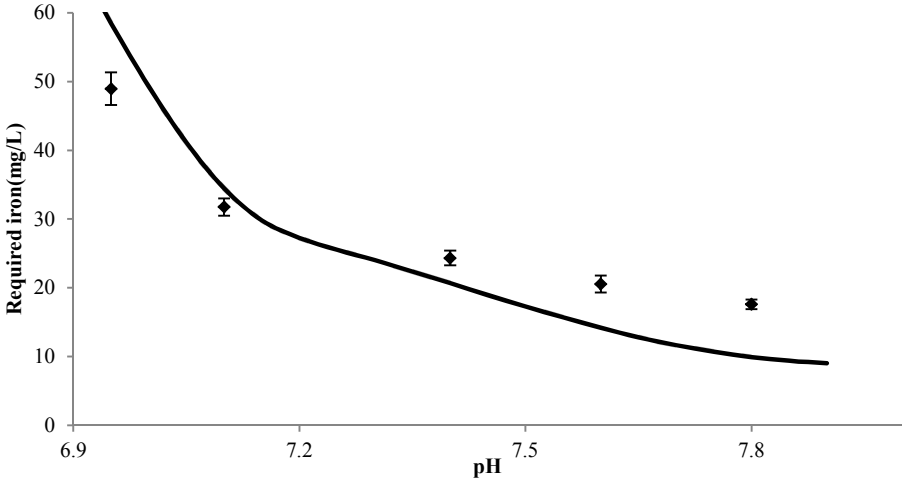

(b)

Figure 2: (a) Fe(II) concentration and (b) Minimum iron required for removal of As(tot) from 500 to < 50 µg/L as a function of pH. Symbols are experimental data. Bars on symbols represent a

range of observations in replicate experiments. The lines represent the output from the model calculation. Charge dosage rate: 3 Coulombs/min/L.

Influence of HCO_3^-/CO_3^{2-}. Inorganic carbon (present primarily as HCO_3^- at near-neutral pH) is a concern in EC systems because it is commonly found in high concentrations in natural groundwater and has been implicated as possibly influencing the kinetics of both Fe(II) and As(III) oxidation[26, 36]. To investigate the influence of HCO_3^-/CO_3^{2-} on As(III) oxidation in the EC system in SBGW, a series of As(III) oxidation experiments were conducted for a range of HCO_3^- concentrations (3 to 50 mM) at pH 7.0. As shown in Figure 3, no clear difference in the behavior of As(III) oxidation is apparent within the range of 3 to 50 mM HCO_3^-, which covers a significant fraction of naturally occurring HCO_3^-/CO_3^{2-} concentrations in groundwater[14]. As described by King et al[36], in 2mM HCO_3^- solutions at 5.5 < pH < 7.5, the Fe(II) species that accounted for the highest fraction (~70%) of total Fe(II) oxidation by both DO and H_2O_2 was $FeCO_3^0$ [36]. Due to the similar concentration of HCO_3^- in SBGW, it is likely that $FeCO_3^0$ is also the dominant Fe(II) species contributing to total Fe(II) oxidation in the EC system at pH 7.0. Accordingly, as long as the concentration of HCO_3^- > 2mM, it is likely that the dominant Fe(II) species will remain $FeCO_3^0$, resulting in very little change in As(III) oxidation behavior. The unchanged behavior of As(III) oxidation at a range of HCO_3^- concentrations suggests that our model can be applied to groundwater of varying HCO_3^- levels.

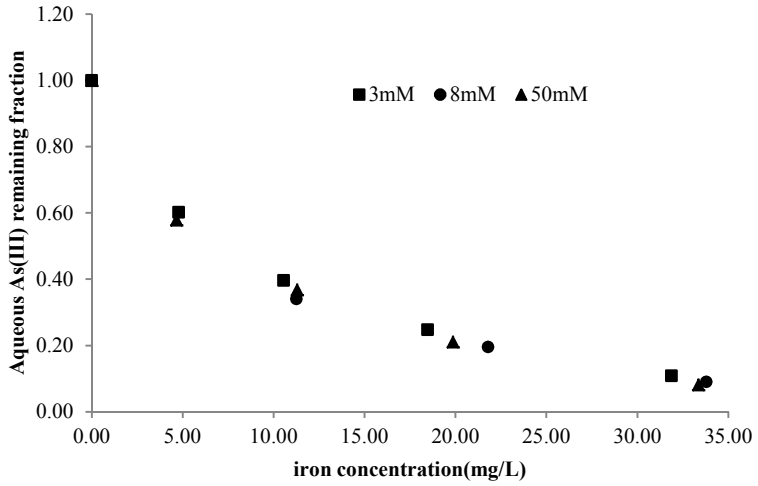

Figure 3: Oxidation of As(III) as a function of bicarbonate and iron concentration. Initial concentrations: 500 μg/L As(III), 3.0 mg/L P, and 30 mg/L Si; initial and final pH 7.0 ± 0.1. Charge dosage rate: 3 Coulombs/L/min. Reaction time: 2h.

Removal of Competing Ions. Figure 4 compares measurements and model predictions for the simultaneous removal of As(III), Si and P in SBGW using EC under a typical charge dosage rate (3 Coulombs/L/min) at pH 7.0. Model predictions agree with experiment well, allowing for a deeper understanding of how these ubiquitous ions behave during EC. At the outset of electrolysis, As(III) is rapidly oxidized to As(V) due to the high $R_{As(III)/Fe(II)}$ at the initial stage. Once oxidized, As(V) is adsorbed rapidly, indicated by the decreasing difference between aqueous As(tot) and aqueous As(III). At the same time, P is rapidly adsorbed. Only after the extensive adsorption of P and As(V) do As(III) and Si begin to be adsorbed at higher total iron concentrations.

Throughout the entire dosing period, the behavior of aqueous As(tot) is nearly identical to that of aqueous As(III), which points to the almost complete and immediate adsorption of As(V) after the oxidation of As(III). Previous authors have reported similar behavior, suggesting that it is due to the absence of As(III) oxidation[16]. We propose that the similar behavior of aqueous As(tot) and As(III) is due to the high extent of As(III) oxidation and extensive, preferential adsorption of As(V), consistent with a previous X-ray absorption spectroscopy study showing direct evidence for As(III) oxidation during EC[38].

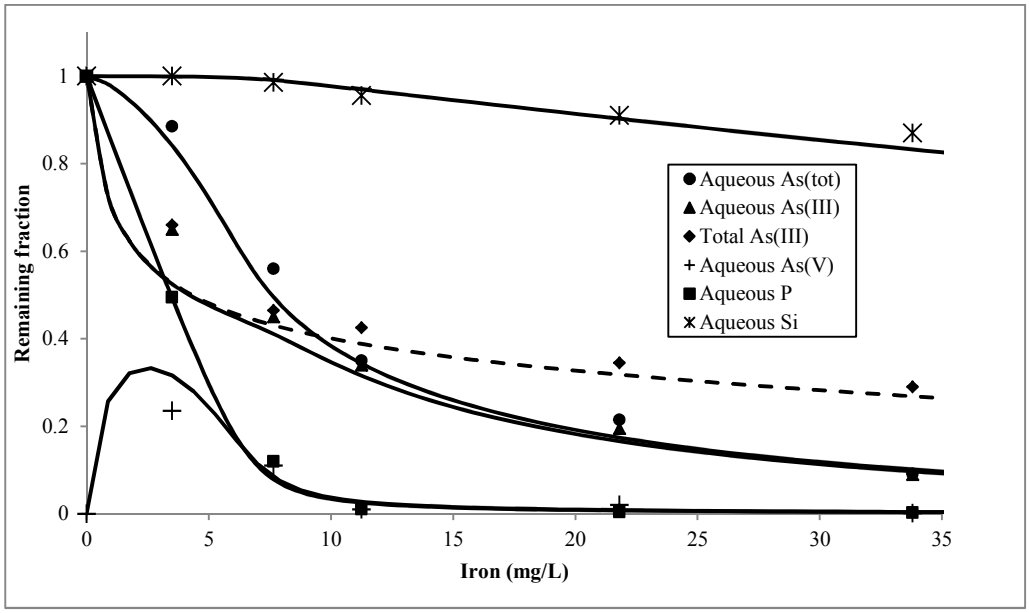

Figure 4: Removal of As(III), As(V), P and Si. The lines represent the output from the model calculation as aqueous (solid) and total (dashed) concentrations. Symbols are experimental data. The lines represent the output from the model calculation. Initial concentrations: 500 μg/L

As(III), 3.0 mg/L P, and 30 mg/L Si; initial and final pH 7.1±0.1. Charge dosage rate: 3 Coulombs/L/min.

Influence of Oxidant Scavengers. Previous work has shown that 2-propanol and As(III) react similarly with $OH^{\bullet}$ (the rate constants for As(III) and 2-propanol oxidation by $OH^{\bullet}$ are $2x10^9$/s and $8x10^9$/s, respectively)[26, 39, 40]. To examine the identity of the As(III) oxidant in the EC system, we added 2-propanol in excess (14 mM) at a pH range of 6.5-8.0. We found negligible effect (within the standard error of the test) of 2-propanol on As(III) oxidation. This is consistent with the As(III) oxidant being an Fe(IV) species generated as an intermediate during the oxidation of Fe(II) in SBGW[26]. As described in previous studies by other investigators, an Fe(IV) species is likely not as reactive as $OH^{\bullet}$, and thus, might selectively react with As(III) in the presence of 2-propanol[28]. It was additionally noted that As(III) oxidation during electrolysis was negligible if Fe(II) oxidation was suppressed by the addition of 3 mM 2,2′-bipyridine, consistent with Katsoyiannis et al.[28] This rules out any potential electrocatalytic reactions that might oxidize As(III) (anodic Cl_2 production or direct anodic As(III) oxidation).

Model Comparison and Application. The reasonably good agreement between experimental data and model predictions for As(III) oxidation and As(III,V) adsorption indicates that our model can be applied to predict As(III,V) removal in SBGW as a function of iron concentration, solution chemistry and/or EC operating parameters. The model is also able to

provide useful predictions of the minimal iron dosage needed for adequate treatment, which is essential to ensure sustainable, low-cost treatment in the field.

However, it should be noted that our model was developed assuming negligible changes in pH during treatment. As we have shown, the removal of As(III) in SBGW is governed by many simultaneous reactions, with several having a strong pH dependence (e.g. Fe(II) oxidation, As(III,V) adsorption). In our experimental data, pH was held constant throughout the electrolysis and reaction stages (see methods section). However, in EC field treatment, it is possible that pH can drift, which can lead to erroneous model predictions of arsenic removal. Therefore, to provide an estimation of the accuracy of our model, we tested our model with experimental data extracted from a notable CC study of As(III) removal in a water matrix similar to SBGW (Figure 5 and 7 of Roberts et al.[14]). As reported in Roberts et al., the pH during the reaction stage varied 0.1-0.4 units above the initial pH value of 7.0+/-0.1, which is somewhat different than the pH maintained in the majority of our study (7.0+/-0.1). The model prediction is compared to experimental data Figure 5. Considering the slightly different solution composition and reaction conditions, the reasonable agreement between the experimental data and our model predictions (Figure 5) suggests that our model is applicable in less rigorously controlled conditions. Nonetheless, to provide the most accurate predictions of As(III) oxidation and As(III,V) removal, and to improve the universality of our model, further work is needed to incorporate modest pH variations during the electrolysis and reaction stages. Model predictions must also be compared to EC performance in real arsenic-contaminated groundwater.

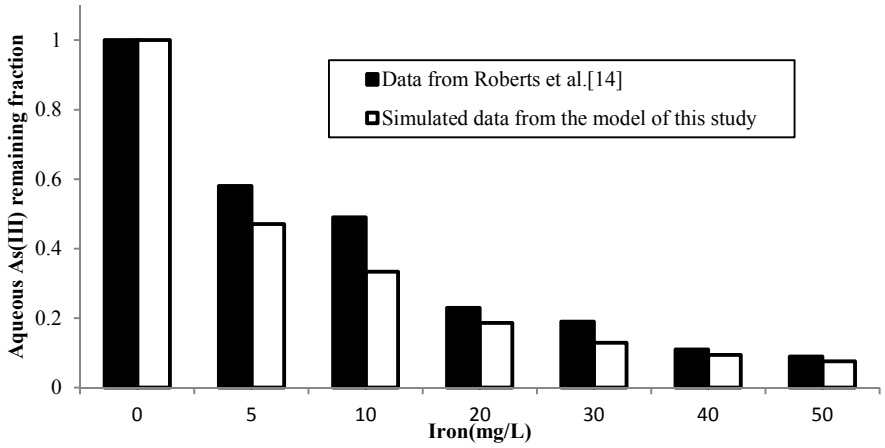

(a)

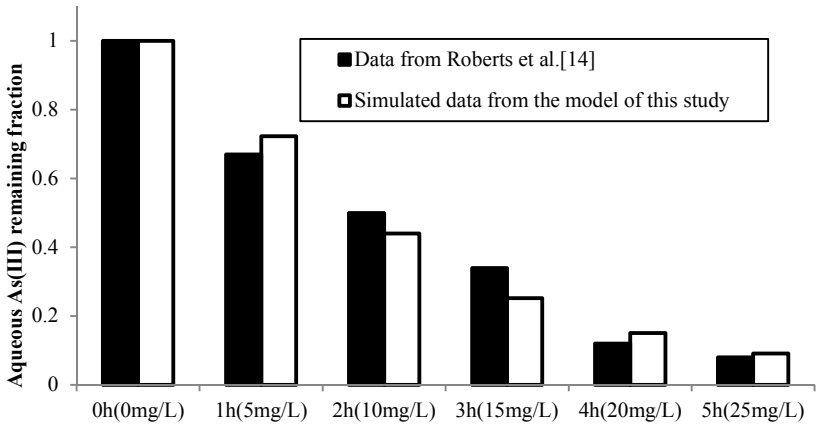

(b)

Figure 5: Comparison of As(III) removal by CC. Experimental data from Roberts et al., 2004[14] (dark solid columns) and model predictions from this study (white columns): (a) Fe(II) addition at time = 0 and (b) hourly additions of 5 mg/L Fe(II). Initial concentrations: 500 μg/L As(III), 3.0 mg/L P, and 30 mg/L Si; pH 7.0.

Supporting Information Available

Supporting information contains a schematic drawing of the experimental setup and details of the determination of reaction constants and model parameters. This information is available free of charge via the Internet at http://pubs.acs.org.

Acknowledgements

We gratefully acknowledge support for this work by The Richard C. Blum Center for Developing Economies, USEPA P3 Phase II award, The Sustainable Products and Solutions Program at Haas School of Business at UC Berkeley, support from the Chinese Scholarship Council to the first author (LL) and an NSF Graduate Research Fellowship to the second author (CVG).

1. Karim, M. M., Arsenic in groundwater and health problems in Bangladesh. *Water Res.* **2000,** *34* (1), 304-310.
2. Farmer, J. G.; Johnson, L. R., Assessment of occupational exposure to inorganic arsenic based on urinary concentrations and speciation of arsenic. *Brit. J. Ind. Med.* **1990,** *47* (5), 342-348.
3. Argos, M.; Kalra, T.; Rathouz, P. J.; Chen, Y.; Pierce, B.; Parvez, F.; Islam, T.; Ahmed, A.; Rakibuz-Zaman, M.; Hasan, R.; Sarwar, G.; Slavkovich, V.; van Geen, A.; Graziano, J.; Ahsan, H., Arsenic exposure from drinking water, and all-cause and chronic-disease mortalities in Bangladesh (HEALS): A prospective cohort study. *Lancet* **2010,** *10*, 60481-60483.
4. WHO, *Guidlines for drinking-water quality*. The World Health Organization: Geneva, Switzerland, 1993.
5. USEPA, *Arsenic treatment technologies for soil, waste and water, Tech. Report no.EPA-542-r-02-004* USEPA: 2002.

6. Kumar, P. R.; Chaudhari, S.; Khilar, K. C.; Mahajan, S. P., Removal of arsenic from water by electrocoagulation. *Chemosphere* **2004,** *55* (9), 1245-1252.

7. Lakshmanan, D.; Clifford, D. A.; Samanta, G., Ferrous and ferric ion generation during electrocoagulation. *Environ. Sci. Technol.* **2009,** *43*, 3853-3859.

8. Barrera-Díaz, C.; Bilyeub, B.; Roaa, G.; Bernal-Martinez, L., Physicochemical aspects of electrocoagulation. *Sep. Purif. Rev.* **2011,** *40* (1), 1-24.

9. Addy, S. E. A. Electrochemical arsenic remediation for rural Bangladesh. Ph.D. Dissertation, University of California - Berkeley, 2008.

10. Holt, P. K., Barton G.W. Mitchell C.A., The future for electrocoagulation as a localised water treatment technology. *Chemosphere* **2005,** *59* (3), 355-367.

11. Chen, G., Electrochemical technologies in wastewater treatment. *Sep. Purif. Technol.* **2004,** *38* (1), 11-41.

12. Mollah, M. Y. A.; Morkovsky, P.; Gomes, J. A. G.; Kesmez, M.; Parga, J.; Cocke, D. L., Fundamentals, present and future perspectives of electrocoagulation. *J. Hazard. Mater.* **2004,** *114* (1-3), 199-210.

13. USEPA, *Technologies and costs for removal of arsenic from drinking water, Tech. Report no.EPA -815-r-00-028*. USEPA: 2000.

14. Roberts, L. C.; Hug, S. J.; Ruettimann, T.; Billah, M. M.; Khan, A. W.; Rahman, M. T., Arsenic removal with Iron(II) and Iron(III) in waters with high silicate and phosphate concentrations. *Environ. Sci. Technol.* **2004,** *38* (1), 307-315.

15. Meng, X.; Bang, S.; Korfiatis, G. P., Effects of silicate, sulfate, and carbonate on arsenic removal by ferric chloride. *Water Res.* **2000,** *34* (4), 1255-1261.

16. Lakshmanan, D.; Clifford, D. A.; Samanta, G., Comparative study of arsenic removal by iron using electrocoagulation and chemical coagulation. *Water Res.* **2010,** *44* (19), 5641-52.

17. Voegelin, A.; Kaegi, R.; Frommer, J.; Vantelon, D.; Hug, S. J., Effect of phosphate, silicate, and Ca on Fe(III)-precipitates formed in aerated Fe(II)- and As(III)-containing water studied by x-ray absorption spectroscopy. *Geochim. Cosmochim. Ac.* **2010,** *74* (1), 164-186.

18. Kinniburgh, D. G.; Smedley, P. L. *Arsenic contamination of groundwater in Bangladesh*; British Geological Survey: Keyworth, U.K., 2001.

19. Zhao, X.; Zhang, B.; Liu, H.; Qu, J., Removal of arsenite by simultaneous electro-oxidation and electro-coagulation process. *J. Hazard. Mater.* **2010,** *184* (1-3), 472-476.

20. Daniel, R.; Prabhakara Rao, A., An efficient removal of arsenic from industrial effluents using electro-coagulation as clean technology option. *Int. J. Environ. Res.* **2012,** *6* (3), 711-718.

21. Lacasa, E.; Canizares, P.; Sáez, C.; Fernández, F. J.; Rodrigo, M. A., Removal of arsenic by iron and aluminium electrochemically assisted coagulation. *Sep. Purif. Technol.* **2011,** *79*, 15-19.

22. Ali, I.; Khan, T. A.; Asim, M., Removal of arsenate from groundwater by electrocoagulation method. *Env. Sci. Pollut. Res.* **2011,** *19* (5), 1668-1676.

23. Mohora, E.; Roncević, S.; Dalmacija, B.; Agbaba, J.; Watson, M.; Karlović, E.; Dalmacija, M., Removal of natural organic matter and arsenic from water by electrocoagulation/flotation continuous flow reactor. *J. Hazard. Mater.* **2012,** *in press*.

24. Lakshmipathiraj, P.; Prabhakar, S.; Raju, G. B., Studies on the electrochemical decontamination of wastewater containing arsenic. *Sep. Purif. Technol.* **2010,** *73* (2), 114-121.

25. Wan, W.; Pepping, T. J.; Banerji, T.; Chaudhari, S.; Giammar, D. E., Effects of water chemistry on arsenic removal from drinking water by electrocoagulation. *Water Res.* **2011,** *45* (1), 384-392.

26. Hug, S. J.; Leupin, O., Iron-catalyzed oxidation of arsenic(III) by oxygen and by hydrogen peroxide; pH-dependent formation of oxidants in the Fenton reaction. *Environ. Sci. Technol.* **2003,** *37* (12), 2734-2742.

27. Voelker, B. M.; Sulzberger, B., Effects of fulvic acid on Fe(II) oxidation by hydrogen peroxide. *Environ. Sci. Technol.* **1996,** *30* (4), 1106-1114.

28. Katsoyiannis, I. A.; Ruettimann, T.; Hug, S. J., pH dependence of Fenton reagent generation and As(III) oxidation and removal by corrosion of zero valent iron in aerated water. *Environ. Sci. Technol.* **2008,** *42* (19), 7424-7430.

29. Bataineh, H.; Pestovsky, O.; Bakac, A., pH-induced mechanistic changeover from hydroxyl radicals to iron(IV) in the Fenton reaction. *Chem. Sci.* **2012,** *3* (5), 1594-1599.

30. Keenan, C. R.; Sedlak, D. L., Ligand-enhanced reactive oxidant generation by nanoparticulate zero-valent iron and oxygen. *Environ. Sci. Technol.* **2008,** *42* (18), 6936--6941.

31. Guan, X.; Ma, J.; Dong, H.; Jiang, L., Removal of arsenic from water: Effect of calcium ions on As(III) removal in the KMnO4-Fe(II) process. *Water Res.* **2009,** *43* (20), 5119-5128.

32. Meng, X. G.; Korfiatis, G. P.; Bang, S. B.; Bang, K. W., Combined effects of anions on arsenic removal by iron hydroxides. *Toxicol. Lett.* **2002,** *133* (1), 103-111.

33. Wolfram Research *Mathematica. Version 7.0 ed*, Wolfram Research, Inc: Champaign, Illinois, 2008.

34. Millero, F. J.; Sotolongo, S.; Izaguirre, M., The oxidation-kinetics of Fe(II) in seawater. *Geochim. Cosmochim. Ac.* **1987,** *51* (4), 793-801.

35. Stumm, W.; Lee, G. F., Oxygenation of ferrous iron. *Ind. Eng. Chem.* **1961,** *53* (2), 143-146.

36. King, D. W.; Farlow, R., Role of carbonate speciation on the oxidation of Fe(II) by H2O2. *Mar. Chem.* **2000,** *70* (1-3), 201-209.

37. Dixit, S.; Hering, J. G., Comparison of arsenic(V) and arsenic(III) sorption onto iron oxide minerals: Implications for arsenic mobility. *Environ. Sci. Technol.* **2003,** *37* (18), 4182-4189.

38. van Genuchten, C. M.; Addy, S. E. A.; Peña, J.; Gadgil, A. J., Removing arsenic from synthetic groundwater with iron electrocoagulation: An Fe and As k-edge EXAFS study. *Environ. Sci. Technol.* **2012,** *46* (2), 986-994.

39. Klaning, U. K.; Bielski, B. H. J.; Sehested, K., Arsenic(IV) - a pulse-radiolysis study. *Inorg. Chem.* **1989,** *28* (14), 2717-2724.

40. Buxton, G. V.; Greenstock, C. L.; Helman, W. P.; Ross, A. B., Critical-review of rate constants for reactions of hydrated electrons, hydrogen-atoms and hydroxyl radicals (.OH/.O-) in aqueous-solution. *J. Phys. Chem. Ref. Data.* **1988,** *17* (2), 513-886.